IOP PUBLISHING PHYSICAL BIOLOGY

Phys. Biol. **7** (2010) 036009 (12pp) doi:10.1088/1478-3975/7/3/036009

Using Jensen's inequality to explain the role of regular calcium oscillations in protein activation

C Bodenstein[1,3], B Knoke[1,4], M Marhl[2], M Perc[2] and S Schuster[1]

[1] Department of Bioinformatics, Friedrich Schiller University Jena, Ernst-Abbe-Platz 2, D-07743 Jena, Germany

[2] Department of Physics, Faculty of Natural Sciences and Mathematics, University of Maribor, Koroška cesta 160, SI-2000 Maribor, Slovenia

E-mail: christian.bodenstein@uni-jena.de and stefan.schu@uni-jena.de

Received 30 June 2010
Accepted for publication 18 August 2010
Published 10 September 2010
Online at stacks.iop.org/PhysBio/7/036009

Abstract

Oscillations of cytosolic Ca^{2+} are very important for cellular signalling in excitable and non-excitable cells. The information of various extracellular stimuli is encoded into oscillating patterns of Ca^{2+} that subsequently lead to the activation of different Ca^{2+}-sensitive target proteins in the cell. The question remains, however, why this information is transmitted by means of an oscillating rather than a constant signal. Here we show that, in fact, Ca^{2+} oscillations can achieve a better activation of target proteins than a comparable constant signal with the same amount of Ca^{2+} used. For this we use Jensen's inequality that describes the relation between the function value of the average of a set of argument values and the average of the function values of the arguments from that set. We analyse the role of the cooperativity of the binding of Ca^{2+} and of zero-order ultrasensitivity, which are two properties that are often observed in experiments on the activation of Ca^{2+}-sensitive target proteins. Our results apply to arbitrary oscillation shapes and a very general decoding model, thus generalizing the observations of several previous studies. We compare our results with data from experimental studies investigating the activation of nuclear factor of activated T cells (NFAT) and Ras by oscillatory and constant signals. Although we are restricted to specific approximations due to the lack of detailed kinetic data, we find good qualitative agreement with our theoretical predictions.

S Online supplementary data available from stacks.iop.org/PhysBio/7/036009/mmedia

List of abbreviations

AECR	array enhanced coherence resonance
CaM kinase II	Ca^{2+}/calmodulin-dependent protein kinase II
ER	endoplasmic reticulum
ERK	extracellular signal-regulated kinase
GEF	guanine nucleotide exchange factor
IP_3	inositol 1,4,5-trisphospate
ISI	interspike interval
MAPK	mitogen-activated protein kinase
NFAT	nuclear factor of activated T cells

[3] Author to whom any correspondence should be addressed.

[4] Present address: Institute of Biochemical Engineering, University of Stuttgart, Allmandring 31, 70569 Stuttgart, Germany.

1. Introduction

The role of intracellular Ca^{2+} oscillations in signal transduction of non-excitable cells, as well as the underlying mechanisms leading to their generation and subsequent evaluation, has been extensively studied experimentally [1–5] and theoretically [6–11]. These oscillations occur due to

an exchange of Ca^{2+} between the cytosol and the endoplasmic reticulum (ER) or other intracellular stores in several types of non-excitable cells such as oocytes, hepatocytes and astrocytes.

The question which physiological advantages Ca^{2+} oscillations have in comparison to adjustable stationary Ca^{2+} levels has often been asked [8, 12–16]. One proposed advantage is the lowering of the average cytosolic Ca^{2+} level by oscillations, since higher concentrations of Ca^{2+} are detrimental for the cell due to precipitation of Ca^{2+} salts or the risk of apoptosis due to Ca^{2+} overloaded mitochondria [17, 18]. This hypothesis of concentration lowering has been confirmed for a specific class of Ca^{2+} models having a net flux of Ca^{2+} across the cell membrane with a constant Ca^{2+} influx and an efflux that only depends on cytosolic Ca^{2+} [19]. It was shown that, when the efflux follows a convex kinetics over the amplitude range of the oscillations, the average Ca^{2+} level is lower or equal to the comparable steady-state level, whereas this is reversed in the case of a concave efflux kinetics.

Due to the observation of unchanged or even increased average Ca^{2+} levels, the question remains how this affects Ca^{2+}-dependent proteins. Prominent examples from this class of proteins are: protein kinase C [20], calcineurin [21], calmodulin [22], and proteins affected by calmodulin such as Ca^{2+}/calmodulin-dependent protein kinase II (CaMKII) [23], myosin light-chain kinase [24] and phosphorylase b kinase [25]. These proteins are able to decode the information contained in an oscillating Ca^{2+} signal. This was shown experimentally for the CaMKII [26] and subsequently analysed in a theoretical study [27]. The information is then relayed to other target proteins, for example by phosphorylation cascades in the case of Ras signalling [28]. Theoretical studies of the decoding of Ca^{2+} signals by Ca^{2+}-sensitive proteins have accompanied these experimental findings [29–33].

Moreover, the advantage of an oscillating compared to a constant signal for the activation of target proteins has been analysed in a number of analytical [33], numerical [15, 34–36] and experimental [28, 37–39] studies. For example, experimentally superimposed oscillations [28, 37–39] or, in theoretical studies, artificial (square-shaped) [33] as well as oscillating signals generated by Ca^{2+}-oscillation models [15, 34–36] were used. Other potential advantages of oscillations have also been discussed cf [8], such as higher robustness against perturbations [40], prevention of receptor desensitization [12] and the possibility to selectively activate target proteins [32, 41, 42]. Here we are interested in elucidating the advantages of oscillations over a constant signal and the role of nonlinear kinetics played therein. Specifically, we focus on the activation of target proteins and study this analytically for arbitrary signals and a generalized decoding model by using Jensen's inequality [43, 44]. The latter provides a well-suited theoretical background in that it describes the relation between the function value of the average and the average of the function values. Jensen's inequality has been used earlier to study other biological questions, such as the importance of environmental variation in ecology [45] or optimal body temperature [46]. An accurate disposition on Jensen's inequality will be given in the following section, whereas in sections 3 and 4 we present the results and discuss their implications, respectively.

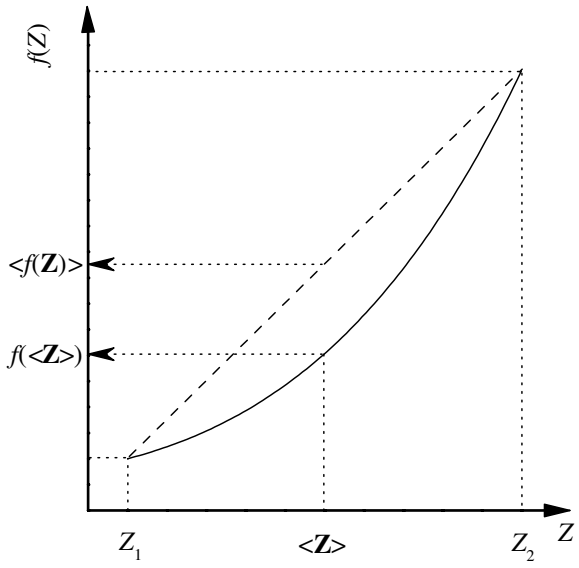

Figure 1. Illustration of Jensen's inequality by using a set **Z** of just two values, Z_1 and Z_2. $f(\langle \mathbf{Z} \rangle)$ is the function value of the averaged argument and $\langle f(\mathbf{Z}) \rangle$ is the average of the two function values. (——) convex function $f(Z)$, (- - - -) line connecting the function values of Z_1 and Z_2 to visualize the average of these function values.

2. Methods

2.1. Jensen's inequality

Jensen's inequality (published in French) [43] is named after the Danish mathematician Johan Jensen. It says that a convex function f has the property that the function value of the average (of two or more) argument values $Z_1, Z_2, \ldots$ forming a set **Z** is not greater than the average of the function values $f(Z_1), f(Z_2), \ldots$ (figure 1 and cf [44]).

For the analysis of Ca^{2+} oscillations the case where **Z** is a continuous interval is relevant. The variable Z is then the cytosolic Ca^{2+} concentration, which is a periodic function over time. For obvious reasons, we consider the average over one period of the oscillation, which can be expressed as an integral over time divided by the oscillation period T:

$$f\left(\frac{1}{T}\int_T Z(t)\,\mathrm{d}t\right) \leqslant \frac{1}{T}\int_T f(Z(t))\,\mathrm{d}t, \qquad (1)$$

with f being convex over an interval **Z** between minimum and maximum values (amplitudes) of the oscillation. Using the short notation for the average $\langle\rangle$ this can be written as

$$f(\langle Z \rangle) \leqslant \langle f(Z) \rangle. \qquad (2)$$

For strictly convex functions the inequality is strict. For concave functions, the opposite holds, with an analogous constraint for strictly concave functions.

The prerequisite of convexity for Jensen's inequality to be true is that the second derivative of $f(Z)$ is non-negative,

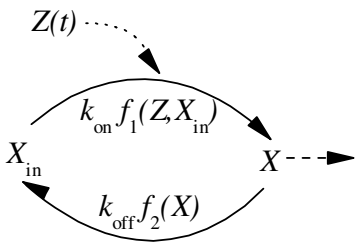

Figure 2. Target protein model: Z, X and X_{in} are the concentrations of Ca^{2+}, active and inactive target protein, respectively. k_{on} and k_{off} are the rate constants of activation and deactivation.

$f''(Z) \geqslant 0$, for all Z in an interval comprising $\mathbf{Z}$. The binding kinetics of Ca^{2+} to proteins are indeed convex functions, at least partly. Jensen's inequality allows us to compare the average protein activation with the activation achieved by a constant signal.

2.2. Model of target protein activation

Here we assume that protein activation by Ca^{2+} spikes can be described by differential equations. We consider an arbitrary Ca^{2+} signal $Z(t) \geqslant 0$ with a period T and amplitude range $[Z_1, Z_2]$. Throughout the study, we assume that the sequestration of Ca^{2+} by the Ca^{2+}-binding proteins is so small that it can be neglected in the Ca^{2+} balance [41]. The time course of the activated form of a target protein, X, can then be written as

$$\frac{dX}{dt} = F(Z, X) = k_{on} f_1(Z, X_{tot} - X) - k_{off} f_2(X) \quad (3)$$

$$= k_{on}(f_1(Z, X_{tot} - X) - K_D f_2(X)), \quad (4)$$

where we have used the conservation relation $X_{tot} = X + X_{in}$ to express the amount of the inactive protein X_{in} (figure 2). Moreover, we have introduced the dissociation constant $K_D = k_{off}/k_{on} > 0$.

The first term describes the Ca^{2+}-dependent activation of X with the maximal turnover rate k_{on}, while the second term describes the Ca^{2+}-independent inactivation of X with the maximal rate k_{off}. Such a model generalizes a wide number of approaches used to model the decoding of Ca^{2+} oscillations [15, 29, 30, 32–34, 36, 42]. We can assume that $F(Z, X)$ is strictly monotonic increasing in $Z > 0$ because Ca^{2+} activates the protein. Moreover, we assume it to be strictly monotonic decreasing in X because of the decay of the activated form and the effect of the conservation relation in the activation process. In particular, we can choose the rate laws such that $f_1 \geqslant 0$ is strictly monotonic increasing in $Z > 0$ and $X_{tot} - X$, and $f_2 \geqslant 0$ is strictly monotonic increasing in X. We can derive some results for such a very general model. Later, we concentrate on functions f_1 that are separable in their arguments:

$$f_1(Z, X_{tot} - X) = v(Z) f_1^*(X_{tot} - X). \quad (5)$$

Usually Ca^{2+} is cooperatively bound to Ca^{2+}-activated proteins. This gives rise to a nonlinear decoding of Ca^{2+} oscillations. For example, up to four Ca^{2+} ions bind to calmodulin, which, in turn, activates CaMKII cf [22]. The term $v(Z) \geqslant 0$ describes the Ca^{2+}-dependent activation by an arbitrary activation function, which could, for example, be a simple mass-action kinetics with molecularity n [42]:

$$v(Z) = Z^n. \quad (6)$$

It could also be a Hill kinetics in Z [30]:

$$v(Z) = \frac{Z^n}{(K_S)^n + Z^n}, \quad (7)$$

where K_S and n are the half-saturation constant and Hill coefficient, respectively. Note that we have omitted the maximal velocities since they are already incorporated in k_{on}. Additionally, f_1^* denotes the binding kinetics of the target protein X to a Ca^{2+}-dependent activator. The functions f_1^* and f_2 could be linear kinetics if (3) models the Ca^{2+}-dependent protein itself or Michaelis–Menten kinetics if X is activated in a phosphorylation cycle by a Ca^{2+}-dependent kinase. Thus, such a modelling comprises different mechanisms proposed for the decoding of Ca^{2+} signals [29, 32, 33]. Examples of models that do not fulfil the separability condition (5) are the ones in [15, 34].

3. Results

3.1. Time courses of the target protein

The steady state X_{ss} for the case of constant Ca^{2+} is given by solving

$$\frac{dX}{dt} = F(Z, X_{ss}(Z)) = 0. \quad (8)$$

Due to $\partial F/\partial X < 0$ for all $Z \in [Z_1, Z_2]$ and $X \in [0, X_{tot}]$, which we assumed in the definition of our model, the implicit function theorem assures that there exists a unique steady-state solution $X_{ss}(Z)$ to (8) [47]. Moreover, since the derivative $\partial F(Z, X)/\partial X$ is negative at the steady state, this state is asymptotically stable in the case of constant Ca^{2+}. In the supporting text, section 2 (available at stacks.iop.org/PhysBio/7/036009/mmedia), we show that this together with $\partial F/\partial Z > 0$ implies that $X_{ss}(Z)$ is strictly monotonic increasing in $Z > 0$ and, in the separable case, $X_{ss}(v(Z))$ is a strictly monotonic increasing function in $v > 0$. Therefore, we can solve 8 in that case:

$$\frac{v(Z)}{K_D} = \frac{f_2(X_{ss})}{f_1^*(X_{tot} - X_{ss})} = h(X_{ss}), \quad (9)$$

$$h^{-1}\left(\frac{v(Z)}{K_D}\right) = X_{ss}(v(Z)). \quad (10)$$

In the supporting text, section 1 (available at stacks.iop.org/PhysBio/7/036009/mmedia), we show by a Poincaré map that the system given in (3) has a unique oscillating solution when forced by an oscillating Ca^{2+} signal $Z(t)$ when $\partial F/\partial X < 0$. This solution also has a period T and the periodic phase will be reached after a certain transient, which is decreasing with k_{on} (cf figure 3).

We are interested whether the oscillations can lead to a stronger activation of the target protein than a comparable constant signal. Here, as a comparable signal, we define a

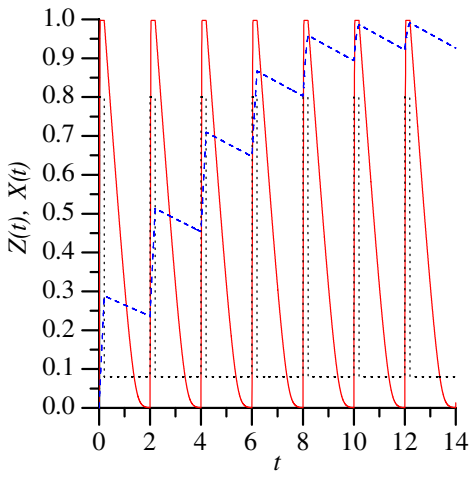

Figure 3. Time course of the underlying Ca^{2+} signal concentration $Z(t)$ (. . . . . , black) and of the active target protein concentration $X(t)$ for different activation constants ($k_{on} = 100$: ——, red; $k_{on} = 4$: - - - -, blue). Here the Ca^{2+} signal is defined as square-shaped spikes in (25) with period $T = 2$, $T_p = 0.2$, $Z_1 = 0.08$ and $Z_2 = 0.8$. The activation kinetics is given by $v(Z) = Z^4$, the total protein concentration is $X_{tot} = 1$ and $K_D = 0.01$. The functions f_1^* and f_2 are described by Michaelis–Menten kinetics with the Michaelis constant 0.1.

constant signal with the same average of Ca^{2+} over one period as the oscillating signal:

$$\bar{Z} = \frac{1}{T}\int_0^T Z(t)\,\mathrm{d}t = \langle Z\rangle. \tag{11}$$

Given this constant input the activated target protein reaches the steady state $X_{ss}(v(\bar{Z}))$ given in (10) and thus we can calculate the average in one period by

$$\langle X_{\bar{Z}}\rangle = X_{ss}(v(\langle Z\rangle)). \tag{12}$$

We will focus here on the case of a separable function f_1 as given in (5), while the derivation for general functions can be found in the supporting text, section 3 (available at stacks.iop.org/PhysBio/7/036009/mmedia). To compute the average of activated protein given an oscillating input we integrate (3) with f_1 separable over one period T:

$$X(T) - X(0) = \int_0^T k_{on}(v(Z) f_1^*(X_{tot} - X) - K_D f_2(X))\,\mathrm{d}t. \tag{13}$$

Now using the fact that $X(t+T) = X(t)$ in the periodic phase, we obtain

$$0 = \int_0^T (v(Z) f_1^*(X_{tot} - X) - K_D f_2(X))\,\mathrm{d}t. \tag{14}$$

This condition must be fulfilled by any periodic solution $X(t)$ of (3).

3.2. Comparison of constant and oscillating signals in the limit cases of slow and fast binding kinetics

It is difficult to derive a solution $X(t)$ fulfilling this condition in the general case. However, we can find two solutions for the two limit cases of a very high activation constant ($k_{on} \to \infty$) and a very low activation constant (k_{on} very small but non-zero).

We start with the first case ($k_{on} \to \infty$) in which the level of activated target protein $X(t)$ reacts very fast to a change in the Ca^{2+} concentration $Z(t)$ and reaches the corresponding steady state $X_{ss}(v(Z(t)))$ nearly immediately. This solution fulfils the condition in (14) since for $X = X_{ss}$ the term in the integral becomes 0 due to (8). The average is given by

$$\langle X_{osc}\rangle = \frac{1}{T}\int_0^T X_{ss}(v(Z(t)))\,\mathrm{d}t = \langle X_{ss}(v(Z))\rangle, \tag{15}$$

with the subscript osc referring to the case where X oscillates.

In the second case of a very low activation constant (k_{on} very small but non-zero), the target protein responds only marginally to a change of Ca^{2+} and slowly integrates the input signal over time. After a certain transient phase, this leads to an oscillating output with small amplitude in the periodic phase. Thus, as an approximation, we can set $X(t) = X_{int}$ in (14) with the subscript int referring to this 'integration case':

$$0 = \int_0^T (v(Z) f_1^*(X_{tot} - X_{int}) - K_D f_2(X_{int}))\,\mathrm{d}t. \tag{16}$$

After dividing by T, rearranging the terms and taking the inverse as in (10) we obtain an expression for X_{int}:

$$X_{int} = h^{-1}\left(\frac{\langle v(Z)\rangle}{K_D}\right) = X_{ss}(\langle v(Z)\rangle). \tag{17}$$

Thus, for the integration case we derive the following average:

$$\langle X_{int}\rangle = X_{ss}(\langle v(Z)\rangle). \tag{18}$$

To analyse whether and under which conditions oscillations lead to a stronger activation of target proteins, we compare the expression for the average of activated target protein in the case of a constant signal in (12) with the above two limit cases. Note the different locations of the brackets indicating the averaging in equations (12), (15) and (18) for the different cases. This implies that for this comparison we can utilize Jensen's inequality (cf section 2.1).

To compare $\langle X_{osc}\rangle$ and $\langle X_{int}\rangle$, we can distinguish two cases depending on the behaviour of X_{ss} in v. Case 1: X_{ss} is a convex function in v over the interval $[v(Z_1), v(Z_2)]$. Then we obtain $\langle X_{int}\rangle \leqslant \langle X_{osc}\rangle$. Case 2: $X_{ss}(v)$ is concave. Then the opposite holds: $\langle X_{osc}\rangle \leqslant \langle X_{int}\rangle$.

In case 1, it suffices to analyse under which conditions the following holds:

$$\langle X_{\bar{Z}}\rangle \leqslant \langle X_{int}\rangle, \tag{19}$$

which is equivalent to

$$X_{ss}(v(\langle Z\rangle)) \leqslant X_{ss}(\langle v(Z)\rangle). \tag{20}$$

From Jensen's inequality we deduce that the convexity of v in Z over the amplitude range $[Z_1, Z_2]$ is a necessary condition for oscillations to be advantageous. It is clear that the two inequalities $\langle X_{\bar{Z}}\rangle \leqslant \langle X_{int}\rangle \leqslant \langle X_{osc}\rangle$ hold, because the composition of two convex, monotonic increasing functions (X_{ss} and v) is again a convex function.

In case 2 we need to analyse when

$$\langle X_{\bar{Z}}\rangle \leqslant \langle X_{osc}\rangle, \tag{21}$$

which is equivalent to

$$X_{ss}(v(\langle Z\rangle)) \leqslant \langle X_{ss}(v(Z))\rangle. \tag{22}$$

This inequality is fulfilled when X_{ss} is convex in Z over the amplitude range of the signal. Unlike above, it is not immediately clear whether the two inequalities $X_{ss}(v(\langle Z\rangle)) \leqslant \langle X_{ss}(v(Z))\rangle \leqslant X_{ss}(\langle v(Z)\rangle)$ hold because now X_{ss} is concave in v. Thus, to achieve the convexity of X_{ss} in Z we need $v''(Z) \geqslant 0$ to compensate at least in part for the concavity of X_{ss} in v. So v needs to be convex in case 2 as well. Therefore, a necessary condition for a better activation of target proteins by an oscillating signal than by a constant signal of the same average is in both cases a convex dependence of the protein activation on the Ca^{2+} level. This is fulfilled, for example, for the mass-action kinetics with molecularity n in (6) for all values of substrate concentrations and for the Hill kinetics with cooperativity n in (7) below the inflection point.

For the non-separable case we derive in the supporting text, section 3 (available at stacks.iop.org/PhysBio/7/036009/mmedia), that in the integration case (small k_{on}) a necessary condition is the convexity of the function F over Z to fulfil the inequality

$$F(\langle Z\rangle, X) \leqslant \langle F(Z, X)\rangle, \tag{23}$$

which guarantees $\langle X_{\bar{Z}}\rangle \leqslant \langle X_{int}\rangle$. This is a generalization of the condition for separable functions f_1 we derived above.

In the oscillatory case a necessary condition is the convexity of the steady-state response X_{ss} over Z to fulfil the inequality

$$X_{ss}(\langle Z\rangle) \leqslant \langle X_{ss}(Z)\rangle, \tag{24}$$

which guarantees $\langle X_{\bar{Z}}\rangle \leqslant \langle X_{osc}\rangle$. This is the same condition derived as above for separable functions f_1. However, in contrast to the separable case, it is not easy to analyse under which conditions the function $X_{ss}(Z)$ is convex. The analysis of sufficient conditions for convexity shows that the convexity of F in Z is again a required condition. Whereas this convexity condition is easy to fulfil, for example by a cooperative binding of Ca^{2+} ions, it is questionable if the other conditions can always be fulfilled. For example, to fulfil another required condition $F_{XX} = k_{on}(\partial^2 f_1/\partial X^2 - K_D \partial^2 f_2/\partial X^2) > 0$ (cf supporting text, section 3 (available at stacks.iop.org/PhysBio/7/036009/mmedia)) over some interval, we would need f_1 to be strictly convex in X and/or f_2 to be strictly concave in X and K_D sufficiently high. Since a cooperative behaviour in the binding of inactive target proteins has not been observed, f_1 cannot be convex in X, but in fact is most likely linear or even concave because of saturation effects. Therefore, at least f_2 needs to be strictly concave in X and K_D should be sufficiently high. However, a high dissociation constant results in a small concentration of the active target protein. In view of these arguments, it seems natural that there will only be a limited range over Z in which the steady-state response $X_{ss}(Z)$ is convex. To determine this range is hard in the general case without specifying the involved kinetics.

3.3. Interpolating the limit cases

Above, we have derived our results only for the limit cases of very low and very high activation constants to ensure analytical tractability. In general, however, it is very difficult to obtain analytic expressions for the average activated target protein $\langle X\rangle$. The derivation of a very general result for arbitrary functions $F(Z, X)$ using a two-dimensional version of Jensen's inequality is possible (cf supporting text, section 4 (available at stacks.iop.org/PhysBio/7/036009/mmedia)). However, for the result to hold it requires that $F(Z, X)$ is a convex function over Z and X. The conditions one derives for the convexity of $F(Z, X)$ are similar to the ones derived for the convexity of the steady-state response $X_{ss}(Z)$ in (24) (cf section 3.2) except that they have to hold over the entire subset $[Z_1, Z_2]$ and $[0, X_{tot}]$. As before it is unlikely that these conditions hold over the whole subset, since this would require a high dissociation constant K_D, which in turn means low active target protein concentration. Therefore, this general result is only applicable under special conditions that are unlikely to be fulfilled.

When the functions f_1^* and f_2 are linear it is possible to derive an expression for $X(t)$, but the involved integrals need the signal to be specified. This can be done by considering a square-shaped signal, which resembles experimentally observed Ca^{2+} spikes [33]. One can then show that the average $\langle X\rangle$ is strictly monotonic decreasing in the activation constant k_{on} (cf the supporting text, section 5 (available at stacks.iop.org/PhysBio/7/036009/mmedia)). In this case the two limit cases can serve as lower and higher bounds and the lower bound, which actually is the oscillation case ($k_{on} \to \infty$), defines the conditions for a better activation of the target protein by oscillations.

But monotonicity of $\langle X\rangle$ in k_{on} is not always the case as can be seen in numerical simulations when using Michaelis–Menten kinetics for f_1^* and f_2 and square-shaped signals (figure 4). The square-shaped T-periodic signal is described mathematically as [27, 32, 33]

$$Z(t) = \begin{cases} Z_2, & \text{if} \quad (t \bmod T) \leqslant T_p \\ Z_1, & \text{else.} \end{cases} \tag{25}$$

Here Z_1 is the resting level. T_p and Z_2 denote the length and height of each Ca^{2+} peak, respectively. Usually, one also defines the duty ratio of the signal as $\gamma = T_p/T$. It is therefore a measure of the narrowness of the Ca^{2+} peaks.

One can observe in figure 4 that the advantage of the oscillating signal compared to the constant signal is huge. For specific values of K_D one obtains a maximum $\langle X\rangle$ in k_{on}. In all simulations with biologically meaningful parameters for the signal we obtained a maximum, which is a hint that we can still use the appropriate limit case at least as a lower bound. In the supporting text, section 6 (available at stacks.iop.org/PhysBio/7/036009/mmedia), we derive analytically the average value $\langle X\rangle$ for a caricature system with Michaelis–Menten kinetics acting nearly saturated and spike-like Ca^{2+} oscillations. The resulting system shows pronounced zero-order ultrasensitivity [48] and similar behaviour as in figure 4. One can derive that for such a system a strictly monotonic average $\langle X\rangle$ in k_{on}, which is the

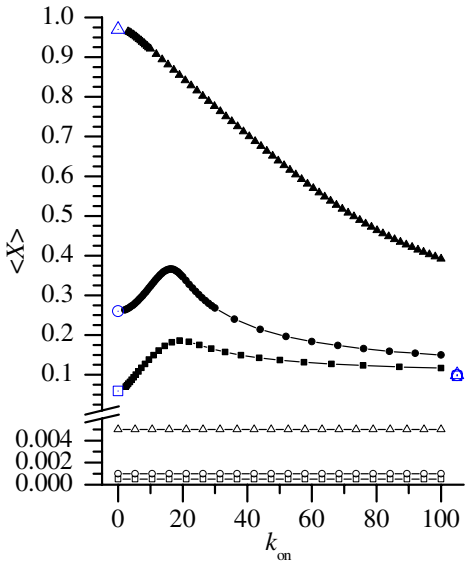

Figure 4. The average target protein activity of $X(t)$ in the periodic phase is plotted over different activation constants k_{on}. Equation (3) is modelled with f_1^* and f_2 described by Michaelis–Menten kinetics with the Michaelis constant 0.1. The activation kinetics is given by $v(Z) = Z^4$ and the total protein concentration is $X_{tot} = 1$. The underlying signal is described by square-shaped spikes with $T = 2$, $T_p = 0.2$, $Z_1 = 0.08$ and $Z_2 = 0.8$. Plotted are the results for different dissociation constants K_D: 0.1 (■), 0.05 (●), 0.01 (▲). The corresponding activation achieved by a constant signal $\bar{Z} = \langle Z \rangle = 0.152$ is indicated by the open symbols. The two derived limit cases for $k_{on} \to 0$ and $k_{on} \to \infty$ are denoted by the (blue) open symbols with a dot.

case when K_D is sufficiently small, is more physiologically relevant.

In the numerical study of the Ca^{2+}-activated liver-glycogen phosphorylase [15] the model is more complicated with a non-separable function f_1. In that study, numerically it was shown that the average is strictly monotonic increasing in the oscillation frequency $\nu = 1/T$ [15, figure 2]. From control analysis of periodically forced oscillations it is known that the following summation theorem holds for time-independent quantities like the average $\langle X \rangle$ [49]:

$$\frac{d\langle X\rangle}{dk_{on}}\frac{k_{on}}{\langle X\rangle} + \frac{d\langle X\rangle}{d\nu}\frac{\nu}{\langle X\rangle} = 0. \tag{26}$$

Since $\nu > 0$, $k_{on} > 0$, $\langle X \rangle > 0$ and from the figure $d\langle X\rangle/d\nu > 0$, we can deduce that $d\langle X\rangle/dk_{on} < 0$ and therefore the average $\langle X \rangle$ is strictly monotonic decreasing in k_{on} at least for the parameter values used in the study [15].

Finally, we note that the two limit cases can be seen as approximations for a wide range of activation constants, and we assume that many of the Ca^{2+}-dependent proteins act in one of the two regimes of oscillations or signal integration.

3.4. Model example

To exemplify the results from section 3.2, we consider an instance of the general model in (3) used in [42]. This minimal model describes the activation and deactivation of a Ca^{2+}-dependent protein X (e.g. CaMKinaseII) by cooperative binding and dissociation of Ca^{2+}:

$$\frac{dX}{dt} = k_{on}(Z^n(X_{tot} - X) - K_D X). \tag{27}$$

In this case we have f_1 separable with a convex activation kinetics $v(Z) = Z^n$ and cooperativity factor $n > 1$. The functions $f_1^* = f_2$ are linear kinetics in their arguments. Since the linear kinetics are monotonic increasing the system reaches a stable and unique periodic phase (cf the supporting text, section 1 (available at stacks.iop.org/PhysBio/7/036009/mmedia)). The stable steady state is given by a Michaelis–Menten-like term increasing in v:

$$X_{ss} = X_{tot}\frac{v(Z)}{K_D + v(Z)}. \tag{28}$$

Moreover, the term is a concave function over the whole positive real space. Thus, this model has the presumably more desired property than $\langle X_{osc} \rangle \leqslant \langle X_{int} \rangle$ for all signals $Z(t)$ with arbitrary amplitude ranges.

Since $v(Z)$ is a convex function we deduce that in the integration case oscillations are always more potent in activating the protein than a constant signal with the same average. In the oscillation case the concentration of the Ca^{2+}-activated protein X is described via a Hill-like term in Z:

$$X(t) = X_{ss}(v(Z(t))) = X_{tot}\frac{Z(t)^n}{(K_S)^n + Z(t)^n}, \tag{29}$$

with the half-saturation constant $K_S = K_D^{1/n}$ and cooperativity n. The Hill kinetics is a sigmoidal curve: it contains convex and concave parts, separated by the point of inflection ($X''(Z_{ip}) = 0$) in the middle which is given by

$$Z_{ip} = K_S\left(\frac{n-1}{n+1}\right)^{1/n}. \tag{30}$$

Obviously, the inflection point is always below the half-saturation constant K_S. The convex contribution in (29) arises from the convexity of the activation kinetics v with $n > 1$. Otherwise, for $n \leqslant 1$ there would be no convex part because then both functions X_{ss} and v are concave. This illustrates the importance of a convex activation kinetics. Since $\langle X_{osc} \rangle \leqslant \langle X_{int} \rangle$, we need to check under which conditions Jensen's inequality holds: $X_{ss}(\langle Z \rangle) \leqslant \langle X_{ss}(Z) \rangle$. Obviously, when the amplitude range is limited by $Z_2 \leqslant Z_{ip}$, the inequality holds for an arbitrary signal because it is restricted to the convex part of (29). This can be achieved by a low Ca^{2+} peak height or a high value for the dissociation constant.

The above conditions on the peak height and dissociation constant can be further specified when the Ca^{2+} signal is similar to square-shaped spikes (cf (25)). As we have shown in a previous study on Ca^{2+} oscillations [19, equation (27)] the Ca^{2+} peak may also extend into the concave part of a Hill kinetics for the inequality in equation (22) to be fulfilled. This crucially depends on narrow Ca^{2+} spikes and very low resting levels between those spikes.

3.5. Comparison with previous studies

3.5.1. Theoretical studies. Our analysis generalizes some of the analytic results obtained in [33]. In that study the response of an instance of our general system in (3) to a square-shaped signal was derived and compared to a constant signal with the same average. To be specific: a separable function f_1 with a Hill kinetics in Ca^{2+} for v and f_1^* and f_2 linear were used. The analysis is similar to ours in section 3.2 in that the limit cases of very low and very high activation constants k_{on} were examined. It was also shown that these limit cases correspond to signals with high and low frequencies, respectively. In the first one the protein cannot react to the signal because the signal frequency is very high and thus the protein integrates the signal, whereas in the second one the frequency is low enough for the protein to adjust its level and therefore to oscillate with the signal. Their analysis emphasized the importance of cooperative Ca^{2+} binding to the Ca^{2+}-dependent protein. However, as we could show here it is the convexity of the kinetics v which is relevant. The results can be well understood in our framework and the critical values obtained there [33, equations (39a) and (40a)] correspond to critical values fulfilling equations (20) and (22) in section 3.2.

Next we compare our results with the numerical study in [36]. The decoding model is essentially the same as the one in [33]; however, the underlying signal is generated by the Li-Rinzel model [50] describing Ca^{2+} oscillations. They compared the activation of target proteins achieved by oscillations with the one achieved by a constant signal with the same average. First, they found out numerically that the mean target activity is increasing with the stimulation level of the second messenger inositol 1,4,5-trisphospate (IP_3). From our analysis this can be explained as follows: the higher the stimulation level, the higher will be the frequency of the Ca^{2+} oscillation, a phenomenon that has been termed frequency encoding [6, 30]. Therefore, the behaviour of the Ca^{2+}-dependent protein will tend from oscillation to the integration of the signal with increasing IP_3 concentration. Because in their model the functions f_1^* and f_2 are linear, the steady state X_{ss} is a concave function of v (cf section 3.4, equation (28)), which implies that the activation achieved in the integration case is higher than in the oscillation case.

Moreover, in the above-mentioned specific model, it was found that without cooperativity in the Ca^{2+}-binding (Hill coefficient $n = 1$) activation by a constant signal with the same average is always better than by an oscillating signal [36]. Note that for $n = 1$ the Hill kinetics $v(Z)$ becomes a concave Michaelis–Menten kinetics. In section 3.2 we have shown that it is necessary for $v(Z)$ to be convex over the signals amplitude range in the oscillation and integration cases. Therefore, without cooperativity the functions $v(Z)$ and $X_{ss}(v(Z))$ are completely concave, which prevents a better activation by oscillations.

In the numerical study by Gall *et al* [15] the activation of the liver glycogen phosphorylase b by Ca^{2+} oscillations was analysed. The specific model is rather complicated with a non-separable function f_1 and a Michaelis–Menten kinetics for f_2. They first analysed the response to artificial sinusoidal oscillations of Ca^{2+} and compared the level of activation with the activation by a constant signal of the same average, which is the same question we study here. However, since experimental Ca^{2+} time courses are for most parts non-sinusoidal, the situation in a full Ca^{2+} model was also numerically analysed in that study. It was found that the activation of the phosphorylase b achieved by oscillations outperforms the activation by a steady-state signal [15, figure 6]. The model used for the generation of Ca^{2+} oscillations in that study has an interesting property. Due to its special stoichiometric structure and a linear efflux kinetics of Ca^{2+} out of the cell, the steady-state Ca^{2+} level Z_{ss} is equal to the average oscillating Ca^{2+}level $\langle Z\rangle$, that means $Z_{ss} = \langle Z\rangle$ [16]. Therefore, the activation of the target protein by the steady-state signal is the same as the activation achieved by a constant signal with the average of the oscillating signal. This property allows us to apply our results. The complexity of the model leads to cumbersome equations. Therefore, we only approximately compare the activation by oscillations and the steady-state signal.

We first compute the amplitude range of the Ca^{2+} signal over the stimulation parameter β using the same model for Ca^{2+} oscillations and parameters as in [15]. For low stimulation levels $\beta \lessapprox 0.2$, which correspond to low-frequency oscillations of Ca^{2+} leading to the oscillation mode of the target protein, the Ca^{2+} oscillations range from $\approx 0.1\,\mu$M to $\approx 0.8\,\mu$M. We need to consider $X_{ss}(Z)$ in the oscillation case, which has an inflection point at $Z_{ip} \approx 0.31\,\mu$M. Although the Ca^{2+} peaks reach comparably far into the concave part of X_{ss}, they do so only for a very small amount of time because of the spike-like Ca^{2+} oscillations with narrow Ca^{2+} peaks that are characteristic for relaxation oscillator models [51]. If we use the square-shaped signal formalism (cf equation (25) for a definition) as an approximation, with $Z_1 = 0.1\,\mu$M and $Z_2 = 0.8\,\mu$M, one can show that the critical inequality (24) is fulfilled for the duty ratio $\gamma = T_p/T$ smaller than 0.25. Such narrow spikes are indeed observed for a low stimulation parameter β. In contrast, high stimulation levels β, which correspond to high-frequency oscillations of Ca^{2+}, lead to the integration of the signal by the target protein. For the integration case, we need to examine the convexity of $f_1(Z, X)$ over the amplitude range of Z. The amplitude range in this case is approximately $[0.2\,\mu\text{M}, 0.6\,\mu\text{M}]$. Using the square-shaped signal formalism and considering this time the critical inequality (23), we derive that it is fulfilled for $\gamma \lessapprox 0.9$. Such or even lower duty ratios are observed for $\beta \geqslant 0.35$. Thus, our analytic results predict the numerical observations.

3.5.2. Experimental studies. An experimental study of our subject using artificially produced Ca^{2+} spikes and measuring the gene expression level achieved by the activation of the transcription factor NFAT in Jurkat T cells was done in [37]. It was found that under low levels of stimulation, which means small Ca^{2+} peaks and a low average level of Ca^{2+}, oscillations enhance the activation of NFAT [37, figure 2(*a*)] compared to a constant signal with the same average. Under high levels of stimulation, however, the constant signal performed better [37, figure 2(*b*)].

To analyse the results in our theoretical framework, we first need to determine how we can effectively model the Ca^{2+}–NFAT signalling system and its relation to the measured gene-expression level. We utilize the results from a related study on the nuclear translocation of exogenous NFAT in baby hamster kidney cells and endogenous NFAT in Jurkat T cells [39]. In that study a model including phosphorylated-cytoplasmic NFAT, dephosphorylated-cytoplasmic NFAT and dephosphorylated-nuclear NFAT, which then initiates gene expression, was fitted to experimental data. The dephosphorylation by the phosphatase calcineurin is the Ca^{2+}-dependent step [21]. Moreover, we assume that the gene expression is directly proportional to the concentration of nuclear NFAT. Although the model includes three variables and a feedback, it can be effectively reduced to a model for only the dephosphorylated-cytoplasmic NFAT. This is due to the conservation relation for the overall NFAT concentration in the cell and the fitted low conversion rate $k_4 = 0.035\ \mathrm{min}^{-1}$ of nuclear NFAT back into the cytoplasmic-phosphorylated NFAT. The latter implies the breaking-up of the feedback and timescale separation such that the nuclear NFAT integrates the concentration changes of the dephosphorylated-cytoplasmic NFAT over time. The integration property was validated experimentally in that study. Therefore, if a periodic Ca^{2+} signal $Z(t)$ controls the dephosphorylation via calcineurin the concentration of the nuclear NFAT N_n is, after an initial transient, approximately given by

$$N_\mathrm{n} = \frac{k_3}{k_4}\langle N_\mathrm{c}\rangle, \tag{31}$$

where N_c is the dephosphorylated-cytoplasmic NFAT and k_3 is the transport rate of N_c into the nucleus. Furthermore, if the kinetics of N_c is linear, as assumed in the fitted model [39] and we assume square-shaped Ca^{2+} spikes, then we have

$$\langle N_\mathrm{c}\rangle \geqslant \langle N_{\mathrm{c,ss}}(Z)\rangle. \tag{32}$$

This is because for linear kinetics we can use the oscillation case as a lower bound for the average protein concentration (cf section 3.3). In contrast, if a constant Ca^{2+} signal with the same average $\langle Z\rangle$ is applied, the steady-state concentration of the nuclear NFAT is given by

$$N_{\mathrm{n,ss}}(\langle Z\rangle) = \frac{k_3}{k_4}N_{\mathrm{c,ss}}(\langle Z\rangle). \tag{33}$$

We want to analyse under which conditions the average nuclear NFAT concentration is higher than the steady-state concentration achieved by a constant Ca^{2+} signal: $N_{\mathrm{n,ss}}(\langle Z\rangle) \leqslant \langle N_\mathrm{n}\rangle$. Equations (31)–(33) imply that to do this it suffices to consider $N_{\mathrm{c,ss}}(\langle Z\rangle) \leqslant \langle N_{\mathrm{c,ss}}(Z)\rangle$. Due to (33) this is equivalent to

$$N_{\mathrm{n,ss}}(\langle Z\rangle) \leqslant \langle N_{\mathrm{n,ss}}(Z)\rangle. \tag{34}$$

Since we assumed the gene expression to be directly proportional to the nuclear NFAT concentration, we can read out $N_{\mathrm{n,ss}}(Z)$ directly from the experimentally measured gene-expression levels under different constant Ca^{2+} concentrations [37, figure (3*a*)].

After having related the measured gene-expression levels to the Ca^{2+}–NFAT signalling system we can analyse the experimental results in [37] using our theoretical approach. The two compared artificial Ca^{2+} signals in the study have different peak heights (i) $Z_2 \approx 0.75\,\mu\mathrm{M}$ and (ii) $Z_2 \approx 1.25\,\mu\mathrm{M}$ and different average values (i) $\langle Z\rangle = 227\,n\mathrm{M}$ and (ii) $\langle Z\rangle = 340\,n\mathrm{M}$, whereas the baseline level $Z_1 \approx 0\ \mu\mathrm{M}$ and the period $T = 100\mathrm{s}$ remain the same. Now we examine the convexity of the steady-state concentration of the nuclear NFAT $N_{\mathrm{n,ss}}(Z)$ over the Ca^{2+} signal's amplitude range. $N_{\mathrm{n,ss}}(Z)$ shows a steep sigmoidal dependence on the Ca^{2+} level and was fitted in their study by a Hill kinetics with $K_\mathrm{S} = 270\,n\mathrm{M}$ and $n = 4.7$ [37, figure (3*a*)], although such a dependence could also be achieved by zero-order ultrasensitivity [48]. Here, we use a Hill kinetics for $N_{\mathrm{n,ss}}$ and apply the square-shaped signal formalism from (25) for the Ca^{2+} spikes. It can then be shown that with the values given in that study for the signal ($Z_1 \approx 0\ \mu\mathrm{M}$, Z_2 and $\langle Z\rangle$) and the Hill coefficient the critical inequality (34) is only fulfilled for (i) $K_\mathrm{S} \gtrapprox 272\,n\mathrm{M}$ and (ii) $K_\mathrm{S} \gtrapprox 420\,n\mathrm{M}$.

The first bound coincides with the K_S value obtained by Dolmetsch *et al* [37] from a fit to the data ($K_\mathrm{S} = 270\,n\mathrm{M}$). Therefore, one would expect that oscillations and a constant signal perform equally well. However, the experimental observations point to a slight advantage of oscillations [37, figure (2*a*)]. This is probably due to the approximative nature of our above analysis, which involves the approximation of the signal by square-shaped spikes and a fitted Hill kinetics to the data for N_ss. On the other hand, the second bound is 1.5 times higher than the fitted K_S value. This means that the Ca^{2+} spike reaches too much into the concave part of the Hill kinetics and the advantage of oscillations is lost. This explains why in the experiments under high levels of stimulation the constant signal outperforms activation by oscillations [37, figure 2(*b*)].

Moreover, in the study by Dolmetsch *et al* the response to oscillatory and constant signals under different average levels of Ca^{2+} $\langle Z\rangle$ was analysed [37, figure 2(*c*)]. It was found out that oscillatory signals outperform constant signals as long as $\langle Z\rangle \lessapprox 300\,n\mathrm{M}$. The different average levels of Ca^{2+} were achieved by adjusting the peak height Z_2, while the duty ratio γ remained constant. To analyse this in our framework, we again use the fitted Hill kinetics for the measured steady-state response $N_{\mathrm{n,ss}}$ [37, figure 3(*a*)]. The inequality (34) with $\langle Z\rangle = \gamma Z_2$ has to hold

$$\frac{\langle Z\rangle^n}{(K_\mathrm{S})^n + \langle Z\rangle^n} \leqslant \gamma\frac{(\langle Z\rangle/\gamma)^n}{(K_\mathrm{S})^n + (\langle Z\rangle/\gamma)^n}. \tag{35}$$

We can rearrange this to obtain an upper bound for $\langle Z\rangle$:

$$\langle Z\rangle \leqslant K_\mathrm{S}\left(\frac{\gamma - \gamma^n}{1-\gamma}\right)^{1/n}. \tag{36}$$

With the parameters given in that study [37]: $\gamma \approx 0.3$, $K_\mathrm{S} = 270\,n\mathrm{M}$ and $n = 4.7$ the upper bound is $\approx 225\,n\mathrm{M}$. This is in good agreement with the experimentally derived upper bound of $\approx 300\,n\mathrm{M}$.

In another experimental study the activation of Ras by Ca^{2+} signals in HeLa cells was studied [28]. Ras is a small protein that interacts with many different signalling pathways in the cell, for example the important extracellular signal-regulated kinase (ERK)/mitogen-activated protein kinase

(MAPK) cascade. Moreover, its conversion to the active GTP-bound form is dependent on Ca^{2+}-regulated proteins [52]. In the experimental study it was shown, as before for NFAT, that oscillations outperform constant Ca^{2+} signals in terms of active Ras–GTP concentration but only under low levels of stimulation with an average level of Ca^{2+} $\langle Z\rangle \lessapprox 400\,n$M [28, figure 2(*b*)]. To analyse this system we first need to ensure that we can apply our theoretical results. Ras cycles between two forms: the inactive GDP-bound form and the active GTP-bound form. The conversion between the inactive and active form depends among others mainly on guanine nucleotide exchange factors (GEFs). These in turn are affected by Ca^{2+}. The conversion between the active into the inactive form is done by GTPase-activating proteins that enhance the intrinsic GTPase activity of Ras. Moreover, the total concentration of Ras remains constant over the timescale of regulation. This allows us to apply our theoretical results to explain the experimental observations. The steady-state concentration of Ras–GTP upon constant stimulation by Ca^{2+} $R_{ss}(Z)$ has been measured in dendrites and spines and shows a sigmoidal dependence on Ca^{2+} that was fitted by a Hill kinetics with $n = 3.1$ and $K_S = 900\,n$M [53]. Due to the lack of more experimental data regarding the detailed kinetics of the Ras–GEF signalling pathway we rely on the steady-state concentration data and analyse the oscillation case where Ras–GTP still oscillates with the Ca^{2+} signal. In analogy to (34) we then have an inequality for $R_{ss}(Z)$. The artificially created spikes in the study by Kupzig *et al* [28] can again be approximated by square-shaped spikes (cf equation (25)) with $Z_1 \approx 0\mu$M and $T = 100$s. To obtain signals with different average concentrations the spike interval and thus the duty ratio γ was kept fixed at $\approx$0.5, while the peak height Z_2 varied. Therefore, we can directly use (36) to obtain an upper bound of $\langle Z\rangle \lessapprox 830\,n$M. The deviation from the experimentally measured value of $\langle Z\rangle \lessapprox 400\,n$M can again be explained by the square-shaped spike approximation and the assumption that Ras–GTP still oscillates with the Ca^{2+} signal.

4. Discussion

Here, we have analysed the effect of oscillations in intracellular Ca^{2+} on the activation of Ca^{2+}-dependent proteins. Jensen's inequality has allowed us to derive analytical results for arbitrary oscillation shapes and a very general decoding model. The main motivation for previous theoretical investigations of this issue [15, 33, 34, 36] was provided by experimental findings that the transcription factor NFAT is activated better by oscillations than by a constant signal with the same average level under low levels of stimulation [28, 37, 39]. Those studies were either numerical [15, 34, 36] or used specific Ca^{2+} signals to be analytically tractable [33]. The general model established here comprises the various models used in those and other studies [30, 42] and uses arbitrary signals. We derived two asymptotic solutions for the oscillation (high activation constant) and integration (low activation constant) cases of the target protein.

In the previous investigations it was found out that a cooperative binding of Ca^{2+} and therefore a nonlinear decoding of the signal is important for oscillations to activate target proteins better [33, 36]. By the use of our general model in (3), which describes the activation of the target protein X by a differential equation, analytically we were able to show that the convexity of the involved kinetics over the amplitude range of the Ca^{2+}signal is crucial. Cooperativity in the binding is only one way of realizing convexity, zero-order ultrasensitivity is another [48]. Our analysis thus extends the studies by Gall *et al* [15] and Zhao *et al* [36] in that the derivation has been done analytically and that of Salazar *et al* [33] in that arbitrary signals have been considered here (while square-shaped signals were used in [33]).

We first compared an arbitrary oscillating signal and a constant signal with the same average. We derived the following conditions under which oscillations outperform constant signals with the same amount of Ca^{2+} in terms of target protein activation: (i) in the integration case (very low activation constant k_{on}) it is necessary that $f_1(Z, X)$ (or equivalently $v(Z)$ when f_1 is separable) shows a convex dependence on the Ca^{2+} concentration, Z, over the amplitude range of the oscillations. This is most likely achieved by a cooperative binding of Ca^{2+} and indeed most of the Ca^{2+}-dependent proteins bind Ca^{2+} cooperatively [33]. This shows the benefit of Ca^{2+} oscillations for the cell, where due to a cooperative Ca^{2+} binding temporarily high Ca^{2+} concentrations achieve a higher level of protein activation. (ii) In the oscillation case (very high activation constant k_{on}) it is necessary that the steady-state Ca^{2+} response X_{ss} shows a convex dependence on the Ca^{2+} concentration over the amplitude range of the oscillations. The convexity of X_{ss} itself is determined by the properties of the decoding system ($F(Z, X)$). A sufficient (and necessary in the case of separable f_1) condition for X_{ss} to be convex at least over part of the amplitude range is again that $f_1(Z, X)$ ($v(Z)$ in the separable case) is convex over Z. However, cooperativity in Ca^{2+} binding is not the only way to achieve a (partly) convex steady-state response X_{ss} as the case of zero-order ultrasensitivity shows. This property, which arises when activation ($f_1(Z, X)$) and deactivation ($f_2(X)$) are operating at saturation with X, has been observed also for Ca^{2+} binding proteins [54, 55]. It allows for extremely convex and concave parts of X_{ss} without the need for a cooperative Ca^{2+} binding. Moreover, by considering specific kinetics for the functions in our model we arrive at conditions relating the amplitude range and parameters of the kinetics. By further specifying the underlying signal we can derive, as a special case, the conditions given in [33, equations (39a) and (40a)].

On comparing our analytical results with the numerical studies [15, 36] we find very good agreement using the kinetics parameters in these studies. The comparison shows that our theoretical results are able to explain the observations of the numerical studies. We also compared our theoretical results with that of experimental studies [28, 37, 39]. Given the approximative estimation of the critical steady-state response of the target proteins and the assumption of square-shaped spikes for the signal we achieved good agreement with our theoretical predictions. Moreover, our study points to the importance of measuring the steady-state response of Ca^{2+}-sensitive proteins to constant Ca^{2+} signals, since these are

important when subsequent levels in the cascade integrate the input. It is also important to measure the time course of target protein activation to decide whether it oscillates with the signal or integrates it.

Our results can be interpreted in the light of the emergence of cooperativity in biological evolution. Since experimental results showed a better activation of target proteins by oscillations under low levels of stimulation, which were confirmed here theoretically, it seems that cooperativity of Ca^{2+} binding and/or zero-order ultrasensitivity have evolved to better distinguish between constant and oscillatory signals. Due to the convex shape of the steady-state active target protein concentration under constant Ca^{2+} levels the active target protein concentration will be very low unless the constant Ca^{2+} signal is above a certain threshold. However, when Ca^{2+} oscillates the Ca^{2+} spikes periodically cross this threshold and achieve a strong activation of the target protein, although the average Ca^{2+} level is still low. This leads to an efficient distinction between constant and oscillatory signals.

It should be noted that recently the stochastic aspect of Ca^{2+} oscillations has gained much interest [11, 56–60]. The Ca^{2+} signal apparently consists of a sequence of random spikes, which is particularly evident by considering the variation of the interspike interval (ISI) [57, 59]. This is due to the spatial and hierarchical organization of events leading to a global Ca^{2+} signal. This organization is mainly influenced by the clustering of IP_3 receptors [61–63] and determines the occurrence of Ca^{2+} blips and puffs [64–67]. Only under a strong coupling of spatially discrete IP_3-receptor clusters, the probability for the nucleation of the next Ca^{2+} wave is high enough to establish an almost regular oscillating system, a mechanism that has been termed array enhanced coherence resonance (AECR) [59, 68–70]. In this context, convexity may also be important to eliminate unwanted stochastic effects on the target protein activation because, due to the random opening of Ca^{2+} channels in unstimulated cells, the steady-state Ca^{2+} concentration fluctuates. In our study we have used arbitrary Ca^{2+} signals with a defined period. Due to the stochastic nature of the Ca^{2+} signals, and especially the ISI, it would be worth extending our analysis also to signals that model the variance in the period in order to assess the effects of stochastic channel opening on target protein activation. A further future direction is the generalization to protein cascades. Here, we have focused on one level of protein activation only. Since, usually, downstream levels do not show cooperativity, oscillations and constant signals would reach the same activation at those levels, as long as there is no feedback to upstream levels. Thus, the existence of cascades is likely to have other functions such as signal amplification [71, 72], band-pass filtering [32] and cross-talk [71].

Acknowledgment

Financial support to CB from the German Ministry of Education and Research (BMBF) in the FORSYS-Partner Initiative is gratefully acknowledged.

References

[1] Woods N M, Cuthbertson K S and Cobbold P H 1986 Repetitive transient rises in cytoplasmic free calcium in hormone-stimulated hepatocytes *Nature* **319** 600–2
[2] Rooney T A, Sass E J and Thomas A P 1989 Characterization of cytosolic calcium oscillations induced by phenylephrine and vasopressin in single fura-2-loaded hepatocytes *J. Biol. Chem.* **264** 17131–41
[3] Berridge M J, Lipp P and Bootman M D 2000 The versatility and universality of calcium signalling *Nat. Rev. Mol. Cell. Biol.* **1** 11–21
[4] Berridge M J, Bootman M D and Roderick H L 2003 Calcium signalling: dynamics, homeostasis and remodelling *Nat. Rev. Mol. Cell. Biol.* **4** 517–29
[5] Thul R, Bellamy T C, Roderick H L, Bootman M D and Coombes S 2008 Calcium oscillations *Adv. Exp. Med. Biol.* **641** 1–27
[6] Goldbeter A 1996 *Biochemical Oscillations and Cellular Rhythms* (Cambridge: Cambridge University Press)
[7] Dupont G, Swillens S, Clair C, Tordjmann T and Combettes L 2000 Hierarchical organization of calcium signals in hepatocytes: from experiments to models *Biochim. Biophys. Acta.* **1498** 134–52
[8] Schuster S, Marhl M and Höfer T 2002 Modelling of simple and complex calcium oscillations: from single-cell responses to intercellular signalling *Eur. J. Biochem.* **269** 1333–55
[9] Falcke M 2004 Reading the patterns in living cells—the physics of Ca^{2+} signaling *Adv. Phys.* **53** 255–440
[10] Dupont G, Combettes L and Leybaert L 2007 Calcium dynamics: spatio-temporal organization from the subcellular to the organ level *Int. Rev. Cytol.* **261** 193–245
[11] Falcke M 2009 Introduction to focus issue: intracellular Ca^{2+} dynamics—a change of modeling paradigm? *Chaos* **19** 037101
[12] Jacob R 1990 Calcium oscillations in electrically non-excitable cells *Biochim. Biophys. Acta.* **1052** 427–38
[13] Heinrich R and Schuster S 1996 *The Regulation of Cellular Systems* (New York: Chapman and Hall)
[14] Putney J W 1998 Calcium signaling: up, down, up, down ... what's the point? *Science* **279** 191–2
[15] Gall D, Baus E and Dupont G 2000 Activation of the liver glycogen phosphorylase by Ca^{2+} oscillations: a theoretical study *J. Theor. Biol.* **207** 445–54
[16] Knoke B, Marhl M, Perc M and Schuster S 2008 Equality of average and steady-state levels in some nonlinear models of biological oscillations *Theory Biosci.* **127** 1–14
[17] Berridge M J 1997 Elementary and global aspects of calcium signalling *J. Exp. Biol.* **200** 315–9
[18] Berridge M J, Bootman M D and Lipp P 1998 Calcium—a life and death signal *Nature* **395** 645–8
[19] Knoke B, Bodenstein C, Marhl M, Perc M and Schuster S 2010 Jensen's inequality as a tool for explaining the effect of oscillations on the average cytosolic calcium concentration *Theory Biosci.* **129** 25–38
[20] Webb B L, Hirst S J and Giembycz M A 2000 Protein kinase C isoenzymes: a review of their structure, regulation and role in regulating airways smooth muscle tone and mitogenesis *Br. J. Pharmacol.* **130** 1433–52
[21] Klee C B, Ren H and Wang X 1998 Regulation of the calmodulin-stimulated protein phosphatase, calcineurin *J. Biol. Chem.* **273** 13367–70
[22] Van Eldik L J and Watterson D M 1998 *Calmodulin and Signal Transduction* (London: Academic)
[23] Colbran R J 2004 Targeting of calcium/calmodulin-dependent protein kinase II *Biochem. J.* **378** 1–16

[24] Stull J T, Tansey M G, Tang D C, Word R A and Kamm K E 1993 Phosphorylation of myosin light chain kinase: a cellular mechanism for Ca^{2+} desensitization *Mol. Cell. Biochem.* **127** 229–37

[25] Brushia R J and Walsh D A 1999 Phosphorylase kinase: the complexity of its regulation is reflected in the complexity of its structure *Front Biosci.* **4** D618–41

[26] Koninck P De and Schulman H 1998 Sensitivity of CaM kinase II to the frequency of Ca^{2+} oscillations *Science* **279** 227–30

[27] Dupont G, Houart G and Koninck P De 2003 Sensitivity of CaM kinase II to the frequency of Ca^{2+} oscillations: a simple model *Cell Calcium* **34** 485–97

[28] Kupzig S, Walker S A and Cullen P J 2005 The frequencies of calcium oscillations are optimized for efficient calcium-mediated activation of Ras and the ERK/MAPK cascade *Proc. Natl Acad. Sci. USA* **102** 7577–82

[29] Goldbeter A, Dupont G and Berridge M J 1990 Minimal model for signal-induced Ca^{2+} oscillations and for their frequency encoding through protein phosphorylation *Proc. Natl Acad. Sci. USA* **87** 1461–5

[30] Dupont G and Goldbeter A 1992 Protein phosphorylation driven by intracellular calcium oscillations: a kinetic analysis *Biophys. Chem.* **42** 257–70

[31] Izu L T and Spangler R A 1995 A class of parametrically excited calcium oscillation detectors *Biophys. J.* **68** 1621–9

[32] Marhl M, Perc M and Schuster S 2005 Selective regulation of cellular processes via protein cascades acting as band-pass filters for time-limited oscillations *FEBS Lett.* **579** 5461–5

[33] Salazar C, Politi A Z and Höfer T 2008 Decoding of calcium oscillations by phosphorylation cycles: analytic results *Biophys. J.* **94** 1203–15

[34] Rozi A and Jia Y 2003 A theoretical study of effects of cytosolic Ca^{2+} oscillations on activation of glycogen phosphorylase *Biophys. Chem.* **106** 193–202

[35] Larsen A Z, Olsen L F and Kummer U 2004 On the encoding and decoding of calcium signals in hepatocytes *Biophys. Chem.* **107** 83–99

[36] Zhao Q, Yi M, Xia K and Zhan M 2009 Information propagation from IP_3 to target protein: a combined model for encoding and decoding of Ca^{2+} signal *Physica* A **388** 4105–14

[37] Dolmetsch R E, Xu K and Lewis R S 1998 Calcium oscillations increase the efficiency and specificity of gene expression *Nature* **392** 933–6

[38] Li W, Llopis J, Whitney M, Zlokarnik G and Tsien R Y 1998 Cell-permeant caged InsP3 ester shows that Ca^{2+} spike frequency can optimize gene expression *Nature* **392** 936–41

[39] Tomida T, Hirose K, Takizawa A, Shibasaki F and Iino M 2003 NFAT functions as a working memory of Ca^{2+} signals in decoding Ca^{2+} oscillation *EMBO J.* **22** 3825–32

[40] Rapp P E, Mees A I and Sparrow C T 1981 Frequency encoded biochemical regulation is more accurate than amplitude dependent control *J. Theor. Biol.* **90** 531–44

[41] Schuster S, Knoke B and Marhl M 2005 Differential regulation of proteins by bursting calcium oscillations—a theoretical study *Biosystems* **81** 49–63

[42] Marhl M, Perc M and Schuster S 2006 A minimal model for decoding of time-limited Ca^{2+} oscillations *Biophys. Chem.* **120** 161–7

[43] Jensen J L W V 1906 Sur les fonctions convexes et les inégalités entre les valeurs moyennes *Acta. Math.* **30** 175–93

[44] Hardy G H, Littlewood J E and Polya G 1952 *Inequalities* 2nd edn (Cambridge: Cambridge University Press)

[45] Ruel J J and Ayres M P 1999 Jensen's inequality predicts effects of environmental variation *Trends. Ecol. Evol.* **14** 361–6

[46] Martin T L and Huey R B 2008 Why 'suboptimal' is optimal: Jensen's inequality and ectotherm thermal preferences *Am. Nat.* **171** E102–E18

[47] Krantz S G and Parks H R 2003 *The Implicit Function Theorem* (Boston: Birkhäuser)

[48] Goldbeter A and Koshland D E 1981 An amplified sensitivity arising from covalent modification in biological systems *Proc. Natl Acad. Sci. USA* **78** 6840–4

[49] Kholodenko B N, Demin O V and Westerhoff H V 1997 Control analysis of periodic phenomena in biological systems *J. Phys. Chem. B* **101** 2070–81

[50] Li Y X and Rinzel J 1994 Equations for InsP3 receptor-mediated $[Ca^{2+}]_i$ oscillations derived from a detailed kinetic model: a Hodgkin-Huxley like formalism *J. Theor. Biol.* **166** 461–73

[51] Schuster S and Marhl M 2001 Bifurcation analysis of calcium oscillations: time-scale separation, canards and frequency lowering *J. Biol. Syst* **9** 291–314

[52] Cullen P J and Lockyer P J 2002 Integration of calcium and Ras signalling *Nat. Rev. Mol. Cell. Biol.* **3** 339–48

[53] Yasuda R, Harvey C D, Zhong H, Sobczyk A, Aelst L van and Svoboda K 2006 Supersensitive Ras activation in dendrites and spines revealed by two-photon fluorescence lifetime imaging *Nat. Neurosci.* **9** 283–91

[54] Meinke M H, Bishop J S and Edstrom R D 1986 Zero-order ultrasensitivity in the regulation of glycogen phosphorylase *Proc. Natl Acad. Sci. USA* **83** 2865–8

[55] Bradshaw J M, Kubota Y, Meyer T and Schulman H 2003 An ultrasensitive Ca^{2+}/calmodulin-dependent protein kinase II-protein phosphatase 1 switch facilitates specificity in postsynaptic calcium signaling *Proc. Natl Acad. Sci. USA* **100** 10512–7

[56] Dupont G, Abou-Lovergne A and Combettes L 2008 Stochastic aspects of oscillatory Ca^{2+} dynamics in hepatocytes *Biophys. J.* **95** 2193–202

[57] Skupin A, Kettenmann H, Winkler U, Wartenberg M, Sauer H, Tovey S C, Taylor C W and Falcke M 2008 How does intracellular Ca^{2+} oscillate: by chance or by the clock? *Biophys. J.* **94** 2404–11

[58] Perc M, Green A K, Dixon C J and Marhl M 2008 Establishing the stochastic nature of intracellular calcium oscillations from experimental data *Biophys. Chem.* **132** 33–8

[59] Skupin A and Falcke M 2009 From puffs to global Ca^{2+} signals: how molecular properties shape global signals *Chaos* **19** 037111

[60] Liao X L, Jung P and Shuai J W 2009 Global noise and oscillations in clustered excitable media *Phys. Rev.* E **79** 041923

[61] Shuai J W and Jung P 2002 Stochastic properties of Ca^{2+} release of inositol 1,4,5-trisphosphate receptor clusters *Biophys. J.* **83** 87–97

[62] Shuai J W and Jung P 2003 Optimal ion channel clustering for intracellular calcium signaling *Proc. Natl Acad. Sci. USA* **100** 506–10

[63] Thul R and Falcke M 2004 Stability of membrane bound reactions *Phys. Rev. Lett.* **93** 188103

[64] Thul R and Falcke M 2006 Frequency of elemental events of intracellular Ca^{2+} dynamics *Phys. Rev.* E **73** 061923

[65] Thul R, Thurley K and Falcke M 2009 Toward a predictive model of Ca^{2+} puffs *Chaos* **19** 037108

[66] Huertas M A and Smith G D 2007 The dynamics of luminal depletion and the stochastic gating of Ca^{2+}-activated Ca^{2+} channels and release sites *J. Theor. Biol.* **246** 332–54

[67] DeRemigio H, LaMar M D, Kemper P and Smith G D 2008 Markov chain models of coupled calcium channels: Kronecker representations and iterative solution methods *Phys. Biol.* **5** 036003

[68] Hu B and Zhou C 2000 Phase synchronization in coupled nonidentical excitable systems and array-enhanced coherence resonance *Phys. Rev.* E **61** R1001–4

[69] Zhou C, Kurths J and Hu B 2001 Array-enhanced coherence resonance: nontrivial effects of heterogeneity and spatial independence of noise *Phys. Rev. Lett.* **87** 098101

[70] Coombes S and Timofeeva Y 2003 Sparks and waves in a stochastic fire-diffuse-fire model of Ca^{2+} release *Phys. Rev.* E **68** 021915

[71] Heinrich R, Neel B G and Rapoport T A 2002 Mathematical models of protein kinase signal transduction *Mol. Cell.* **9** 957–70

[72] Chaves M, Sontag E D and Dinerstein R J 2004 Optimal length and signal amplification in weakly activated signal transduction cascades *J. Phys. Chem.* B **108** 15311–20